The crystal structure of tin sulphate, $SnSO_4$, and comparison with isostructural $SrSO_4$, $PbSO_4$, and $BaSO_4$

Sytle M. Antao[a)]
Department of Geoscience, University of Calgary, Calgary, Alberta T2N 1N4, Canada

(Received 7 February 2012; accepted 3 March 2012)

The crystal structure of tin (II) sulphate, $SnSO_4$, was obtained by Rietveld refinement using synchrotron high-resolution powder X-ray diffraction (HRPXRD) data. The structure was refined in space group *Pbnm*. The unit-cell parameters for $SnSO_4$ are $a = 7.12322(1)$, $b = 8.81041(1)$, $c = 5.32809(1)$ Å, and $V = 334.383(1)$ Å^3. The average ⟨Sn–O⟩ [12] distance is 2.9391(4) Å. However, the Sn^{2+}cation has a pyramidal [3]-coordination to O atoms and the average ⟨Sn–O⟩ [3] = 2.271(1) Å. If Sn is considered as [12]-coordinated, $SnSO_4$ has a structure similar to barite, $BaSO_4$, and its structural parameters are intermediate between those of $BaSO_4$ and $PbSO_4$. The tetrahedral SO_4 group has an average ⟨S–O⟩ [4] = 1.472(1) Å in $SnSO_4$. Comparing $SnSO_4$ with the isostructural $SrSO_4$, $PbSO_4$, and $BaSO_4$, several well-defined trends are observed. The radii, rM, of the M^{2+}(=Sr, Pb, Sn, and Ba) cations and average ⟨S–O⟩ distances vary linearly with *V* because of the effective size of the M^{2+}cation. Based on the trend for the isostructural sulphates, the average ⟨Sn–O⟩ [12] distance is slightly longer than expected because of the lone pair of electrons on the Sn^{2+}cation.
 [doi:10.1017/S0885715612000450]

Key words: $SnSO_4$, $SrSO_4$, $PbSO_4$, $BaSO_4$, Rietveld refinement, HRPXRD, crystal structure

I. INTRODUCTION

The crystal structure of tin (II) sulphate was determined by Rentzeperis (1962) based on the suggestion of James and Wood (1925) that $SnSO_4$ has a barite structure. However, Donaldson and Moser (1960) indicated that such a relation is unlikely because of the large difference in the ionic radii of Ba^{2+} and Sn^{2+} [$r_{Ba} = 1.61$ Å (Shannon, 1976); $r_{Sn} = 0.85$ Å (Donaldson and Puxley, 1972)]. Using single-crystal data, the structure of $SnSO_4$ was refined by Donaldson and Puxley (1972). The main structural features of $SnSO_4$ are illustrated (Figure 1). A lone pair of electrons of the sp^3 hybridized Sn^{2+} orbitals may explain the high degree of distortion in $SnSO_4$ and its relation to the barite structure. In $SnSO_4$, the Sn^{2+} atom is in a pyramidal coordination that forms three bonds with the O atoms and the fourth orbital in the sp^3 hybridization is occupied by a lone pair of electrons [Figure 1(a)]. The lone pair of electrons is viewed as pseudo-ligands, which prevents close approach of other anions in this direction and significantly changes the space requirements (Gillespie, 1967; Gillespie and Robinson, 1996). Crystal structures that have cations with a lone pair of electrons are quite open and they undergo pressure-induced phase transitions (Crichton *et al.*, 2005; Hinrichsen *et al.*, 2008).

The crystal structure of celestite, anglesite, and barite was recently refined by Antao (2012), and interesting structural trends were observed across the series. Miyake *et al.* (1978) indicated a possible systemic variation in the SO_4 tetrahedron with field strength of the M^{2+} cation across the series. Jacobsen *et al.* (1998) concluded that the average ⟨M–O⟩ distance increases linearly with unit-cell volume, but SO_4 behaves as a rigid group with an average ⟨S–O⟩ distance of about 1.476 Å, which is constant across the series. Hawthorne and Ferguson (1975) and Hill (1977) reported that the SO_4 groups in all three structures display identical geometries. These studies indicate that the M^{2+} cations have no effect on the shape or size of the SO_4 tetrahedron. The M^{2+} cations have different sizes and effective charge, so systematic variation in the geometry of the SO_4 group across the series is expected, and this was recently confirmed by Antao (2012). Although the structure of the isostructural MSO_4 materials is well known, previous studies have not shown the change in the geometry of the SO_4 group observed by Antao (2012) using high-resolution powder X-ray diffraction (HRPXRD), which is the same technique used in this study to examine the structure of $SnSO_4$.

The purpose of this study is to refine the crystal structure of $SnSO_4$ and to examine its relation to the structural trends that were recently observed by Antao (2012) for the isostructural sulphates $SrSO_4$, $PbSO_4$, and $BaSO_4$. Of particular interest is the variation in the geometry of the SO_4 group for these sulphates and the radius of the [12]-coordinated Sn^{2+} cation.

II. EXPERIMENTAL

A. Synchrotron HRPXRD

The $SnSO_4$ sample was studied by HRPXRD that was performed at beamline 11-BM, Advanced Photon Source (APS), Argonne National Laboratory (ANL). The synthetic tin (II) sulphate, $SnSO_4$, was obtained as 99% reagent grade powder from ACROS organics, and the HRPXRD trace showed no impurity phase. The sample was crushed to a fine powder using an agate mortar and pestle. The powder sample was loaded into a Kapton capillary (0.8 mm internal diameter) and rotated during the experiment at a rate of 90 rotations per second. The data were collected to a maximum 2θ of about 43° with a step size of 0.001° and a step time of 0.1 s per step. The HRPXRD trace was collected with 12 silicon (111) crystal analysers that increase detector efficiency,

a)Author to whom correspondence should be addressed. Electronic mail: antao@ucalgary.ca

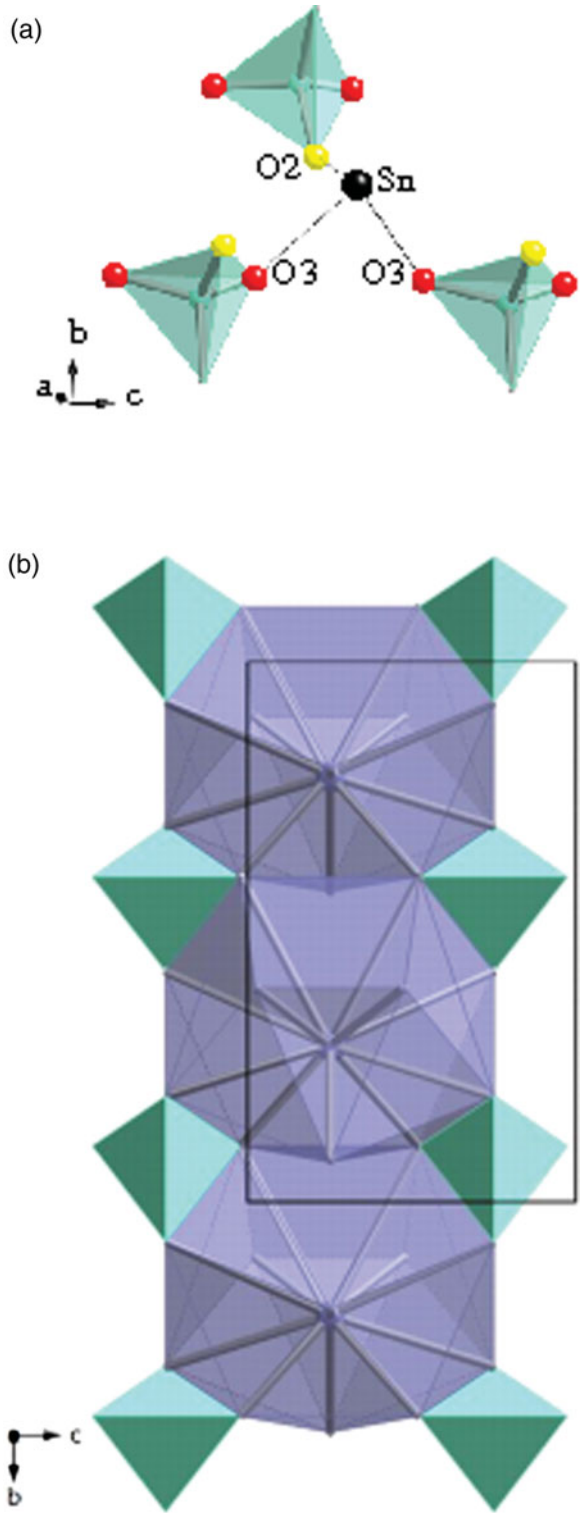

Figure 1. (a) Projection of the $SnSO_4$ structure showing the pyramidal [3]-coordination of a Sn atom to three O atoms of three different SO_4 groups. (b) Sharing of SO_4 and SnO_{12} polyhedral edges in the $SnSO_4$ structure that are the same as in the $BaSO_4$ structure.

reduce the angular range to be scanned, and allow rapid acquisition of data. A silicon (NIST 640c) and alumina (NIST 676a) standard (ratio of ⅓ Si :⅔ Al_2O_3) was used to calibrate the instrument and to refine the monochromatic wavelength [0.41399(2) Å] used in the experiment. Additional details of the experimental set-up are given elsewhere (Antao *et al.*, 2008; Lee *et al.*, 2008; Wang *et al.*, 2008).

B. Rietveld structure refinement

The HRPXRD data were analysed by the Rietveld method (Rietveld, 1969), as implemented in the *GSAS* program (Larson and Von Dreele, 2000), and using the *EXPGUI* interface (Toby, 2001). Scattering curves for ionized atoms were used in the refinement. The starting atom coordinates, unit-cell parameters, and space group *Pbnm* were taken from Donaldson and Puxley (1972). Pure $SnSO_4$ formula was used in the structure refinement. The background was modeled using a Chebyschev polynomial (12 terms). The reflection-peak profiles were fitted using type 3 profile in the *GSAS* program. Full-matrix least-squares refinements were carried out by varying the parameters in the following sequence: a scale factor, unit-cell parameters, atom coordinates, and isotropic displacement parameters. Towards the end of the refinement, all the parameters were allowed to vary simultaneously, and the refinement proceeded to convergence. The fitted HRPXRD trace is shown in Figure 2.

The unit-cell parameters and the Rietveld refinement statistics are listed in Table I. Atom coordinates and isotropic displacement parameters are given in Table II. Bond distances and angles are given in Table III.

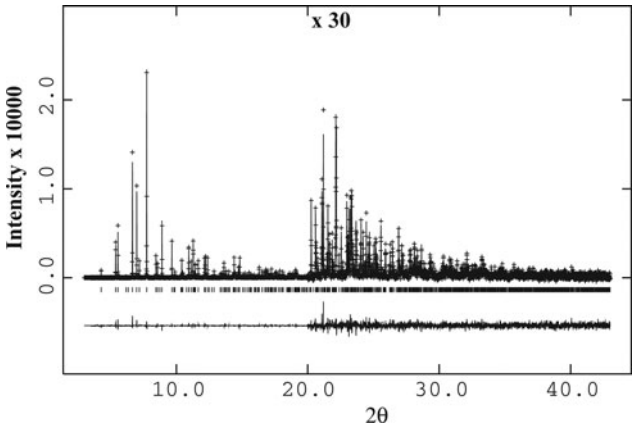

Figure 2. The HRPXRD trace for $SnSO_4$ together with the calculated (continuous line) and observed (crosses) profiles. The difference curve ($I_{obs} - I_{calc}$) is shown at the bottom and has the same scale as that for intensity. The short vertical lines indicate allowed reflection positions. The intensity beyond 20 °2θ is scaled by a factor of ×30. The FWHM of the strongest (121) peak at 7.75 °2θ is 0.009°.

Table I. Unit-cell parameters and Rietveld refinement statistics for $SnSO_4$.

	$SnSO_4$
a (Å)	7.12322(1)
b (Å)	8.81041(1)
c (Å)	5.32809(1)
V (Å^3)	334.383(1)
λ (Å)	0.41399(2)
[a]R (F^2)	0.0581
χ^2	1.276
N_{obs}	1081
N_{data}	39499
2θ range	3.5–43°

[a]R (F^2) = R-structure factor based on observed and calculated structure amplitudes = $[\sum(F_o^2-F_c^2)/\sum(F_o^2)]^{1/2}$. Space group is *Pbnm*; the number of formula units per cell, $Z = 4$.

https://doi.org/10.1017/S0885715612000450 Published online by Cambridge University Press

Table II. Atom positions and isotropic displacement parameters (×100 Å^2) for $SnSO_4$.

	x	*y*	*z*	*U*
Sn	0.21637(4)	0.20970(3)	1/4	2.03(1)
S	0.1806(1)	0.4218(1)	3/4	0.57(2)
O1	0.1049(3)	0.5736(3)	3/4	2.15(7)
O2	0.0323(3)	0.3044(3)	3/4	1.20(5)
O3	0.2982(2)	0.3972(2)	0.9761(2)	1.24(4)

Table III. Selected distances (Å) and angles (°) in $SnSO_4$.

Bonds/angles		
Sn–O2	×1	2.254(2)
Sn–O3	×2	2.280(1)
⟨Sn–O⟩ [3]		2.271(1)
Sn–O1	×1	2.980(2)
Sn–O2	×2	3.084(1)
Sn–O3	×2	3.118(1)
Sn–O1	×2	3.187(1)
Sn–O3	×2	3.348(1)
⟨Sn–O⟩ [12]		2.939(1)
O2–Sn–O3	×2	77.56(5)
O3–Sn–O3	×1	79.61(7)
S–O1	×1	1.442(2)
S–O2	×x1	1.479(2)
S–O3	×2	1.483(1)
⟨S–O⟩ [4]		1.472(1)
O1–S–O2	×1	112.4(1)
O1–S–O3	×	110.3(1)
O2–S–O3	×2	107.5(1)
O3–S–O3	×1	108.7(1)
⟨O–S–O⟩ [6]		109.4(1)

III. RESULTS AND DISCUSSION

The Sn atom is in a pyramidal coordination and is bonded to three O atoms from different SO_4 groups [Figure 1(b)]. If the Sn^{2+} cation is coordinated to 12 O atoms, then the $SnSO_4$ structure is similar to the $BaSO_4$ structure [Figure 1 (b)].

Donaldson and Puxley (1972) refined the structure of $SnSO_4$ in space group *Pnma*, and they concluded that the radius of the Sn atom is too small (they used 0.85 Å) to form a stable $BaSO_4$-type structure. Although they mentioned that $SnSO_4$ and $BaSO_4$ are not isostructural, they indicated that $SnSO_4$ could be considered as a highly distorted form of the barite structure with the Sn atom surrounded by 12 O atoms, as in barite.

In this study, the structure of $SnSO_4$ was refined in space group *Pbnm*, the same as that for barite, and the results are similar to those obtained by Donaldson and Puxley (1972). [Note that space group *Pnma* and *Pbnm* are the same (#62) in different settings. So, structural data from one space group can easily be transformed to the other]. Three of the O atoms are close to an Sn atom [$1 \times 2.254(2)$ and 2×2.280 (1) Å; ⟨Sn–O⟩ = 2.271(1) Å] and the other O atoms are further away [≥2.980(2) Å]. The Sn atom is in a pyramidal three coordination and the pyramidal bond angles are $2 \times 77.56(5)$ and $1 \times 79.61(7)°$ [Figure 1(a) and Table III]. The Sn atom environment was explained in terms of covalent bonding involving sp^3 hybridization of the Sn (II) orbitals (Donaldson and Puxley, 1972). In the sp^3 hybridization, the Sn atom forms three covalent bonds to O atoms and the fourth orbital is occupied by a lone pair of electrons, which prevents close approach of other O atoms in this direction, and gives rise to an open structure. Moreover, the O–Sn–O bond angles of 77.56 and 79.61° obtained in this study agree with the bond-pair and lone-pair repulsion arguments predicting that the O–Sn–O angles are less than 109.5°. The SO_4 group in $SnSO_4$ has a distorted tetrahedral geometry with S–O bond lengths of $1 \times 1.442(2)$, $1 \times 1.479(2)$, and $2 \times 1.483(1)$ Å, and the average ⟨S–O⟩ distance is 1.472(1) Å, compared to 1.487(5) Å obtained by Donaldson and Puxley (1972).

A. Structural trends among $SrSO_4$, $PbSO_4$, $SnSO_4$, and $BaSO_4$

The relevant structural parameters for the isostructural materials are given in Table IV together with the bond–valence sums around the M and S cations and the three independent O atoms. The valence sums for the S cation is close to the expected value of six for all four sulphate compounds. However, the expected valence sum value of two is only observed for the Sr cation and deviates the most for the Sn

Table IV. Comparison of structural parameters for the isostructural sulphates.

	$SrSO_4$	$PbSO_4$	$SnSO_4$	$BaSO_4$
a (Å)	6.87032(3)	6.95802(1)	7.12322(1)	7.15505(1)
b (Å)	8.36030(5)	8.48024(3)	8.81041(1)	8.88101(3)
c (Å)	5.34732(1)	5.39754(1)	5.32809(1)	5.45447(1)
V (Å^3)	307.139(3)	318.486(1)	334.383(1)	346.599(1)
⟨M–O⟩ [12]	2.827(1)	2.865(1)	2.939(1)	2.953(1)
⟨S–O⟩ [4]	1.480(1)	1.477(3)	1.472(1)	1.471(1)
⟨O–S–O⟩ [6]	109.5(1)	109.4(1)	109.4(1)	109.46(3)
*r_M (Å)	1.44	1.49	1.56	1.61
§$\sum M$ (v.u.)	2.08	1.84	1.57	2.21
§$\sum$S (v.u.)	5.92	5.97	6.04	6.06
§$\sum$O1 (v.u.)	−2.02	−1.91	−1.76	−1.97
§$\sum$O2 (v.u.)	−1.91	−2.02	−2.00	−1.98
§$\sum$O3 (v.u.)	−2.03	−1.94	−1.93	−2.16

Data for $SrSO_4$, $PbSO_4$, and $BaSO_4$ are taken from Antao (2012).
*These values and the radii for O^{2-}[4] = 1.38 Å are from Shannon (1976), so r_{Sn} = 2.939–1.38 = 1.56 Å. Bond valence sums (v.u. = valence units) around the M, S, and O atoms were calculated using the program VaList (Wills and Brown, 1999).

https://doi.org/10.1017/S0885715612000450 Published online by Cambridge University Press

cation. The valence sums around the O atoms (especially O1) deviate the most from the expected value of −2.0 for $SnSO_4$, whereas the values for the other compounds are not unreasonable (Table IV).

The radii of 12-coordinated M^{2+} cations, r_M (Shannon, 1976), and the *a*, *b*, *c* unit-cell parameters are plotted against the volume, *V* (Figure 3). The trend lines shown in Figures 3–5 are based only on data from Antao (2012) to which the SnO_4 data are compared, but the $SnSO_4$ data are not included in the computation of the trend lines. The unit-cell parameters *a*, *b*, and *V* for $SnSO_4$ are intermediate between those for $PbSO_4$ and $BaSO_4$, but the *c* parameter is similar to that for $SrSO_4$ (Figure 3). The r_M increases linearly with increasing unit-cell *V* [Figure 3(d)]. The increase in unit-cell parameters arises from the increase in size of the M^{2+} cation. A radius of 1.56 Å was deduced for a [12]-coordinated Sn^{2+} cation (see Table IV).

The average ⟨M–O⟩ [12] distance is plotted against *V* (Figure 4). Linear trends are observed for the data from Antao (2012), but the average ⟨Sn–O⟩ distance is offset from the predicted value based on the trend lines (Figure 4), and is larger because of the lone pair of electrons that causes the SnO_{12} polyhedra to be quite open.

The interesting aspect of this study is the geometrical features of the SO_4 group that are plotted against *V* and r_M (Figure 5). The average ⟨S–O⟩ distance decreases linearly with *V* [Figure 5(a)], whereas the average ⟨O–S–O⟩ angle is constant with *V* (Table IV). The average ⟨S–O⟩ distance decreases linearly with increasing r_M [(Figure 5(c)]. The structural parameters for these isostructural minerals are correlated with the effective size of the M^{2+} cation. In $SrSO_4$, the small Sr^{2+} cation forms a short average ⟨Sr–O⟩ distance so the charge on the O atoms is less and the average ⟨S–O⟩ distance is longer, whereas in $BaSO_4$, the large Ba^{2+} cation forms a longer average ⟨Ba–O⟩ distance so the charge on the O atoms is more and the average ⟨S–O⟩ distance is shorter (Figures 4 and 5). The change in the average ⟨S–O⟩ distances parallels the change in valence sums around the S cation (Table IV). The SO_4 group does not have a rigid-body character, as was previously suggested by Jacobsen *et al.* (1998).

The average ⟨S–O⟩ and ⟨M–O⟩ distances are consistent with expected variations. However, the bond-strength sums around the M cations and O atoms are not consistent (Table IV); but those around the S cations are consistent.

This study shows that in the isostructural sulphate minerals, several well-defined structural trends are observed.

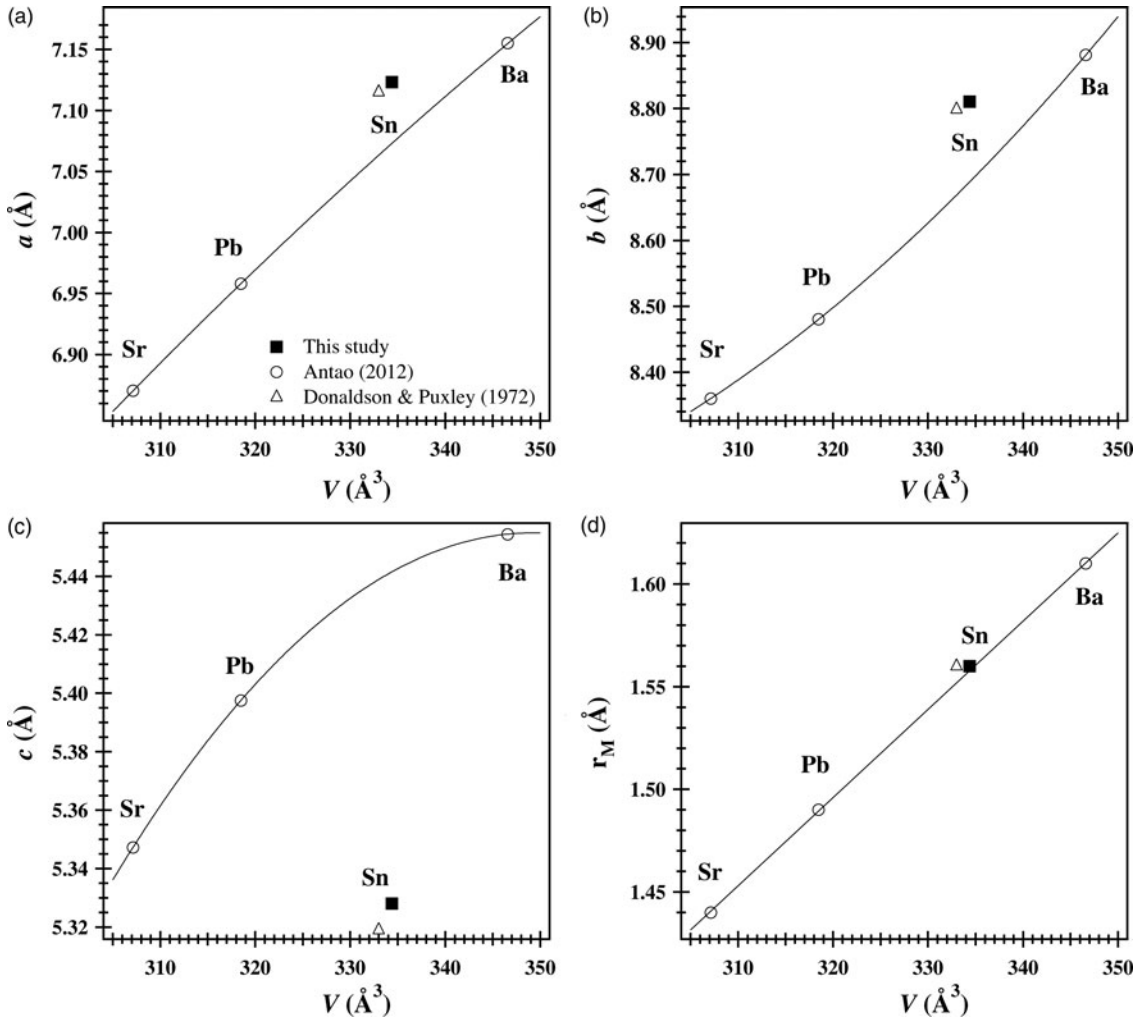

Figure 3. The *a*, *b*, *c* unit-cell parameters and radii of the [12]-coordinated M^{2+} cations, r_M, vs. volume, *V*, for the isostructural sulphates. The unit-cell parameters for $SnSO_4$ are intermediate between $PbSO_4$ and $BaSO_4$. The radii, r_M, increase linearly with *V*. Error bars are smaller than the symbols in Figure 3 and 4. In Figure 3–5, the data for $SnSO_4$ are plotted but they are not included in the computation of the least-squares fitted trend lines.

https://doi.org/10.1017/S0885715612000450 Published online by Cambridge University Press

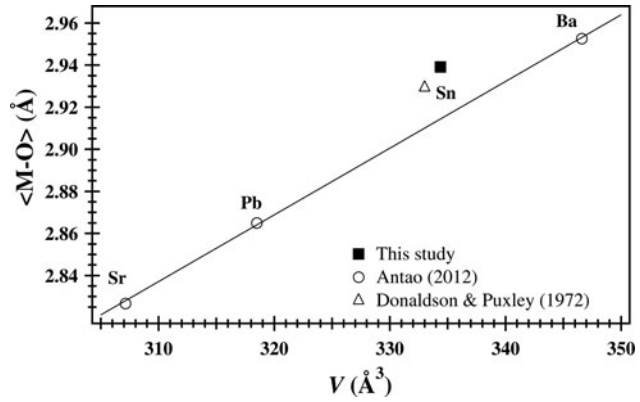

Figure 4. Linear increase in average ⟨M–O⟩ distance with volume, *V*, for the [12]-coordinated M-site in the isostructural sulphates. Data for $SnSO_4$ are close to the trend line for the other sulphates.

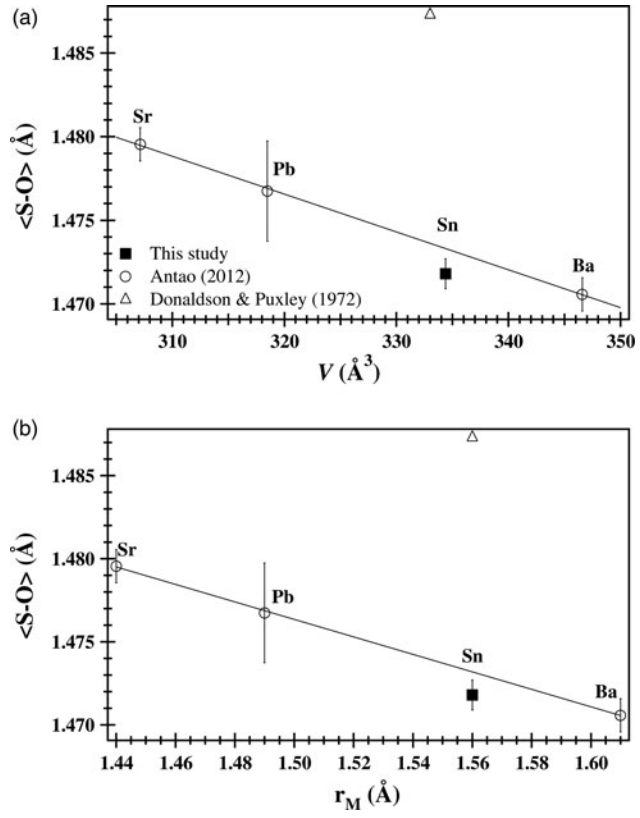

Figure 5. Structural variations of: (a) average ⟨S–O⟩ vs. *V*, and (b) average ⟨S–O⟩ vs. radius of [12]-coordinated M cation, r_M. Data for $SnSO_4$ are close to the linear trends for the other sulphates.

Of particular interest is the geometry of the SO_4 group that changes in a regular manner, as expected. Moreover, the average ⟨S–O⟩ distance in anhydrite [$CaSO_4$; ⟨S–O⟩ = 1.4848(3) Å] is expected to be longer than that in celestite [$SrSO_4$; ⟨S–O⟩ = 1.480(1) Å], which was recently confirmed (Antao, 2011, 2012). Similar results were observed for the orthorhombic carbonates (Antao and Hassan, 2009), where the geometry of the CO_3 group changes in a regular manner. In addition, for the SiO_4 group in framework silicates, the geometry also changes in a regular manner (Antao *et al.*, 2008). Such expected structural trends were not previously observed.

ACKNOWLEDGEMENT

The HRPXRD data were collected at the X-ray Operations and Research beamline 11-BM, APS, and ANL. Use of the APS was supported by the U.S. Department of Energy, Office of Science, Office of Basic Energy Sciences, under Contract No. DE-AC02-06CH11357. This work was supported with a Discovery grant from NSERC and an Alberta Ingenuity Award.

Antao, S. M. (**2011**). "Crystal-structure analysis of four mineral samples of anhydrite, $CaSO_4$, using synchrotron high-resolution powder X-ray diffraction data," Powder Diffr. **26**, 326–330.

Antao, S. M. (**2012**). "Structural trends for celestite ($SrSO_4$), anglesite ($PbSO_4$), and barite ($BaSO_4$): confirmation of expected variations within the SO_4 groups," Am. Mineral. **97**, 661–665.

Antao, S. M. and Hassan, I. (**2009**). "The orthorhombic structure of $CaCO_3$, $SrCO_3$, $PbCO_3$, and $BaCO_3$: linear structural trends," Can. Mineral. **47**, 1245–1255.

Antao, S. M., Hassan, I., Wang, J., Lee, P. L. and Toby, B. H. (**2008**). "State-of-the-art high-resolution powder X-ray diffraction (HRPXRD) illustrated with Rietveld structure refinement of quartz, sodalite, tremolite, and meionite," Can. Mineral. **46**, 1501–1509.

Crichton, W. A., Parise, J. B., Antao, S. M., and Grzechnik, A. (**2005**). "Evidence for monazite-, barite-, and $AgMnO_4$ (distorted barite)-type structures of $CaSO_4$ at high pressure and temperature," Am. Mineral. **90**, 22–27.

Donaldson, J. D. and Moser, W. (**1960**). J. Chem. Soc. 4000–4003.

Donaldson, J. D. and Puxley, D. C. (**1972**). "The crystal structure of tin (II) sulphate," Acta Cryst. **B28**, 864–867.

Gillespie, R. J. (**1967**). "Electron-pair repulsions and molecular shape," Angew. Chem. **79**, 885–896.

Gillespie, R. J. and Robinson, E. A. (**1996**). "Electron-domains and the VSEPR model of molecular geometry," Angew. Chem. **108**, 539–560.

Hawthorne, F. C. and Ferguson, R. B. (**1975**). "Anhydrite sulphates. II. Refinement of the crystal structure of anhydrite," Can. Mineral. **13**, 289–292.

Hill, R. J. (**1977**). "A further refinement of the barite structure," Can. Mineral. **15**, 522–526.

Hinrichsen, B., Dinnebier, R. E., Liu, H., and Jansen, M. (**2008**). "The high pressure crystal structure of tin sulphate: a case study for maximal information recovery from 2D powder diffraction data," Z. Kristallogr. **223**, 195–203.

Jacobsen, S. D., Smyth, J. R., Swope, R. J. and Downs, R. T. (**1998**). "Rigid-body character of the SO_4 groups in celestine, anglesite and barite," Can. Mineral. **36**, 1053–1060.

James, R. W. and Wood, W. A. (**1925**). "The crystal structures of barytes, celestine, and anglesite," Proc. R. Soc. **A109**, 598–620.

Larson, A. C. and Von Dreele, R. B. (**2000**). *General Structure Analysis System* (GSAS). Report No. LAUR 86-748, Los Alamos National Laboratory, Los Alamos, NM.

Lee, P. L., Shu, D., Ramanathan, M., Preissner, C., Wang, J., Beno, M. A., Von Dreele, R. B., Ribaud, L., Kurtz, C., Antao, S. M., Jiao, X. and Toby, B. H. (**2008**). "A twelve-analyzer detector system for high-resolution powder diffraction," J. Synch. Rad. **15**, 427–432.

Miyake, M., Minato, I., Morikawa, H., Iwai, S.-I (**1978**). "Crystal structures and sulphate force constants of barite, celestite, and anglesite," Am. Mineral. **63**, 506–510.

Rentzeperis, P. J. (**1962**). "The crystal structure of the anhydrous stannous sulphate," Z. Kristallogr. **117**, 431.

Rietveld, H. M. (**1969**). "A profile refinement method for nuclear and magnetic structures," J. Appl. Crystallogr. **2**, 65–71.

Shannon, R. D. (**1976**). "Revised effective ionic radii and systematic studies of interatomic distances in halides and chalcogenides," Acta Cryst. **A32**, 751–767.

Toby, B. H. (**2001**). "EXPGUI, a graphical user interface for GSAS," J. Appl. Crystallogr. **34**, 210–213.

Wang, J., Toby, B. H., Lee, P. L., Ribaud, L., Antao, S. M., Kurtz, C., Ramanathan, M., Von Dreele, R. B. and Beno, M. A. (**2008**). "A dedicated powder diffraction beamline at the advanced photon source: commissioning and early operational results," Rev. Sci. Instrum. **79**, 085105.

Wills, A. S. and Brown, I. D. (**1999**). *VaList*. CEA, France. This is a freely available computer program.